

ELEMENTAL COMPOSITION BEFORE, DURING, AND AFTER THE JANUARY 6, 1997, CME EVENT MEASURED BY CELIAS/SOHO

P. Wurz¹, F.M. Ipavich², A.B. Galvin², P. Bochsler¹, M.R. Aellig¹, R. Kallenbach¹, D. Hovestadt³, H. Grünwaldt⁴, M. Hilchenbach⁴, W.I. Axford⁴, H. Balsiger¹, A. Bürgi^{3,†}, M.A. Coplan², J. Geiss^{1,‡}, F. Gliem⁵, G. Gloeckler², S. Hefti¹, K.C. Hsieh⁶, B. Klecker³, M.A. Lee⁷, S. Livi⁴, G.G. Managadze⁸, E. Marsch⁴, E. Möbius⁷, M. Neugebauer⁹, K.U. Reiche⁵, M. Scholer³, M.I. Verigin⁸, and B. Wilken⁴

¹Physikalisches Institut, University of Bern, CH-3012 Bern, Switzerland

²Dept. of Physics and Astronomy and IPST, University of Maryland, College Park, MD 20742, USA

³Max-Planck-Institut für extraterrestrische Physik, Garching, D-85740, Germany

⁴Max-Planck-Institut für Aeronomie, Katlenburg-Lindau, D-37189, Germany

⁵Institut für Datenverarbeitungsanlagen, Technische Universität, D-38023 Braunschweig, Germany

⁶Department of Physics, University of Arizona, Tucson, AZ 85721, USA

⁷EOS, University of New Hampshire, Durham, NH 03824, USA

⁸Institute for Space Physics, Moscow, 117810, Russia

⁹Jet Propulsion Laboratory, Pasadena, CA 91103, USA

ABSTRACT

Using solar wind particle data from the CELIAS experiment on the SOHO mission, we derived densities of the elements O, Ne, Mg, Si, S, Ca, and Fe, and analyzed their abundance before, during, and after the January 6, 1997, coronal mass ejection event. In the inter-stream and coronal hole regions before and after this event we found typical solar wind abundances for the elements investigated. However, during the passage of the CME and during the passage of the erupted filament the elemental composition differed markedly from typical solar wind. For the passage of the CME and for the passage of the erupted filament a mass-dependent enhancement of the elements was found, with a monotonic increase toward heavier elements. We observed Si/O and Fe/O ratios of the order of one during these time periods.

INTRODUCTION

In this paper we present the analysis of the elemental composition of the coronal mass ejection (CME) which originated on January 6, 1997, on the solar surface and arrived at the SOHO spacecraft on January 10, 1997, at 04:10:35 UT. Approximately 30 minutes after the CME passed the SOHO spacecraft, it arrived at the location of the WIND spacecraft. From the WIND measurements it has been concluded that this CME falls into the group of magnetic cloud events [Burlaga, 1997], which make up about a third of all CMEs. We studied the elements O, Ne, Mg, Si, S, Ca, and Fe.

The CME was slightly faster than the preceding solar wind and created a shock which was observed on SOHO on January 10, 1997, at 00:21:35 UT. The CME was followed by coronal hole type solar wind, which arrived at the position of the SOHO spacecraft on January 11 at 06:56 UT. Just before the arrival of the coronal hole a pronounced increase in the proton density was observed, which was attributed to an erupting fila-

[†] Current address: ARIAS, Falkenhöheweg 8, CH-3012 Bern, Switzerland

[‡] Current address: International Space Science Institute, Hallerstrasse 6, CH-3012 Bern, Switzerland

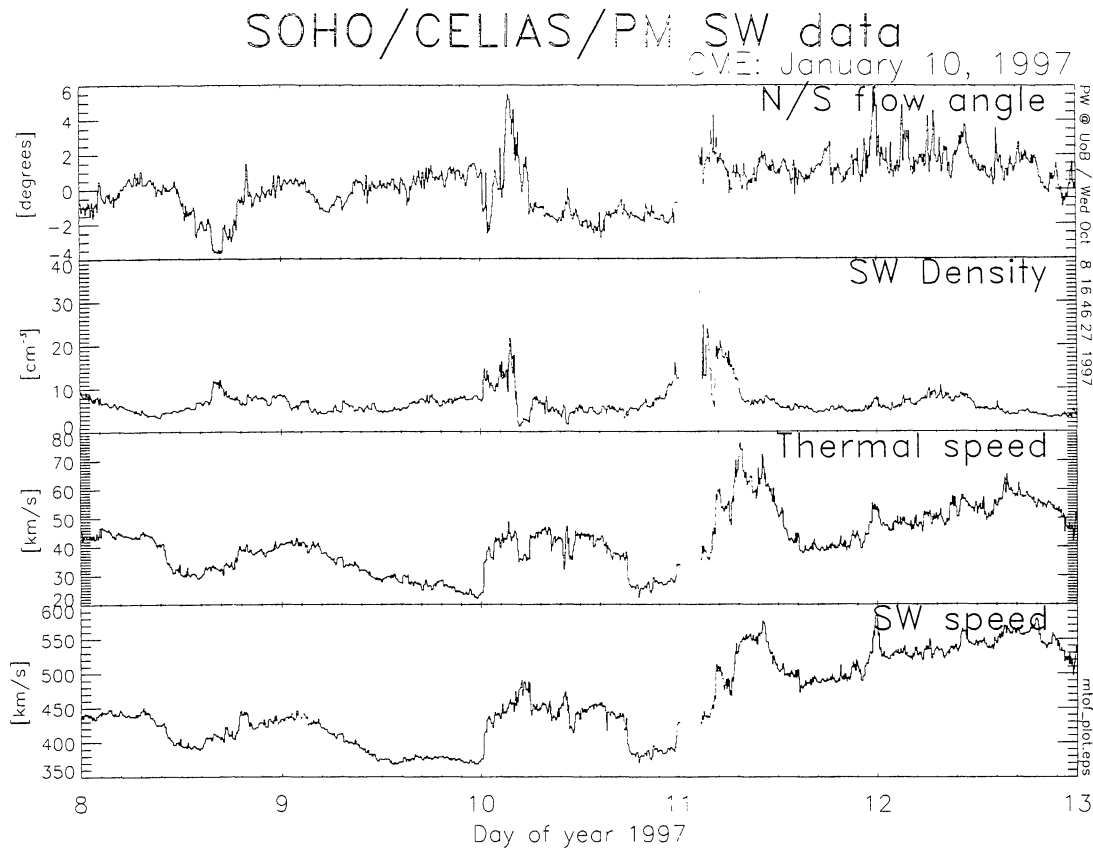


Figure 1: Solar wind plasma parameters as they are measured with the proton monitor, a sensor of the CELIAS instrument on SOHO, are shown for the time period of interest for this study.

ment on the solar surface [Burlaga, 1997]. Together with the time periods before and after the CME passage, this event offers a good opportunity to compare its elemental composition with the two forms of “regular” solar wind composition, originating either from the streamer belt (also called interstream or slow solar wind) or solar wind originating from coronal holes (also called fast solar wind).

The measurements were taken with the MTOF sensor (the Mass Time-of-Flight sensor) of the CELIAS (Charge, Element, and Isotope Analysis System) instrument on the SOHO spacecraft, which is located at the L1 libration point between Earth and Sun. The MTOF sensor is an isochronous time-of-flight (TOF) mass spectrometer [Hamilton *et al.*, 1990] utilizing the carbon foil technique, combined with an electrostatic entrance system [Hovestadt *et al.*, 1995]. The entrance system allows ions to enter the sensor in a large energy range (only discriminating against protons, and partly against alpha particles) and through a wide angular acceptance cone. The MTOF sensor determines the mass of incoming ions with high mass resolution, sufficient to identify many isotopes and rare elements in the solar wind.

We measured the solar wind plasma parameters, namely the solar wind speed, thermal speed, proton density, and N/S solar wind flow angle, with the proton

monitor (PM), which is part of the CELIAS instrument. From these solar wind plasma parameters, for which the interesting time interval is shown in Figure 1, the exact times of the passages of the shock, the CME, the filament, and the coronal hole associated solar wind were identified. Due to saturation of the PM, the proton density spike from the filament eruption could not be measured correctly. WIND/SWE results indicate that the proton density was about 120 cm^{-3} in the spike resulting from the filament eruption, which is about a factor of 10 more than in slow solar wind.

DATA ANALYSIS

Data collected by the MTOF sensor of the CELIAS instrument on the SOHO spacecraft were used for this analysis. The CELIAS instrument and its sensors, among them the MTOF and the PM, has been described in detail by Hovestadt *et al.* [1995]. From the ions recorded with the MTOF sensor, the CELIAS data processing unit accumulated time-of-flight (TOF) spectra for 5 minutes, which then were transmitted to ground. Mass peaks for the different elements were extracted from each of these TOF spectra. Subsequently, the overall efficiency of the MTOF sensor was calculated for each element and for each accumulation interval. To obtain

densities of the indicated elements, the instrument response of the MTOF sensor, which comprises the response of the entrance system and the transmission of the isochronous TOF mass spectrometer, was taken into account in great detail, and was evaluated at the actual solar wind plasma parameters which were measured by the PM (see in Figure 1). By applying the instrument function to the measured data, absolute densities for the different elements were derived. Although the determination of the solar wind plasma parameters from the PM is very accurate [Ipavich *et al.*, 1997], this precision is actually not needed for a precise determination of absolute densities with the MTOF sensor. Absolute errors for the determination of elemental densities were estimated to be between 5% and 10% for the elements considered in this study. The MTOF instrument settings, which are cycled, and have been optimized for a broad range of solar wind conditions. In principle, a time resolution of five minutes can be obtained if the sensitivity of the MTOF sensor is high enough for the particular element considered. For typical solar wind conditions, it is indeed possible to derive densities with this high time resolution for the more abundant elements in the solar wind, as will be shown later in this paper.

RESULTS AND DISCUSSION

The densities derived from the measured data for the elements O, Ne, Mg, Si, S, Ca, and Fe are shown in Figure 2 for the interesting time period around the CME event. What can be seen already from Figure 2 without detailed analysis is that the compressed region after the shock had larger densities than the preceding interstream solar wind. This was also observed for the filament eruption, where a substantial increase in density was observed for that period. Table 1 gives a detailed analysis of the densities and Table 2 gives abundance ratios relative to oxygen for the different periods during the CME event. The time periods for the shock, the CME and the filament are indicated by the gray background in Figure 2. To derive the density for the interstream regime, the data accumulated during DOY 8 (day of year) has been evaluated. For the density in the coronal hole associated solar wind data from the time period after the stream interface until the end of DOY 12 has been evaluated. The stream interface was identified according to [Burlaga, 1974] through a decrease in proton density by a factor of about 2 and an accompanying two-fold increase in kinetic temperature.

Before we go into the details of the CME event itself, we first discuss the unperturbed solar wind, in the interstream regime (the slow solar wind) and in the coronal hole regime (the fast solar wind). The abundance of elements was highly variable with time. Usually averages over long time periods have been performed to give reliable ratios of elemental abundances. Since we focused on the analysis of the CME event, we only used an integration period of about one day for the analysis of the unperturbed solar wind. We found that the abundance of elements with low first ionization potential

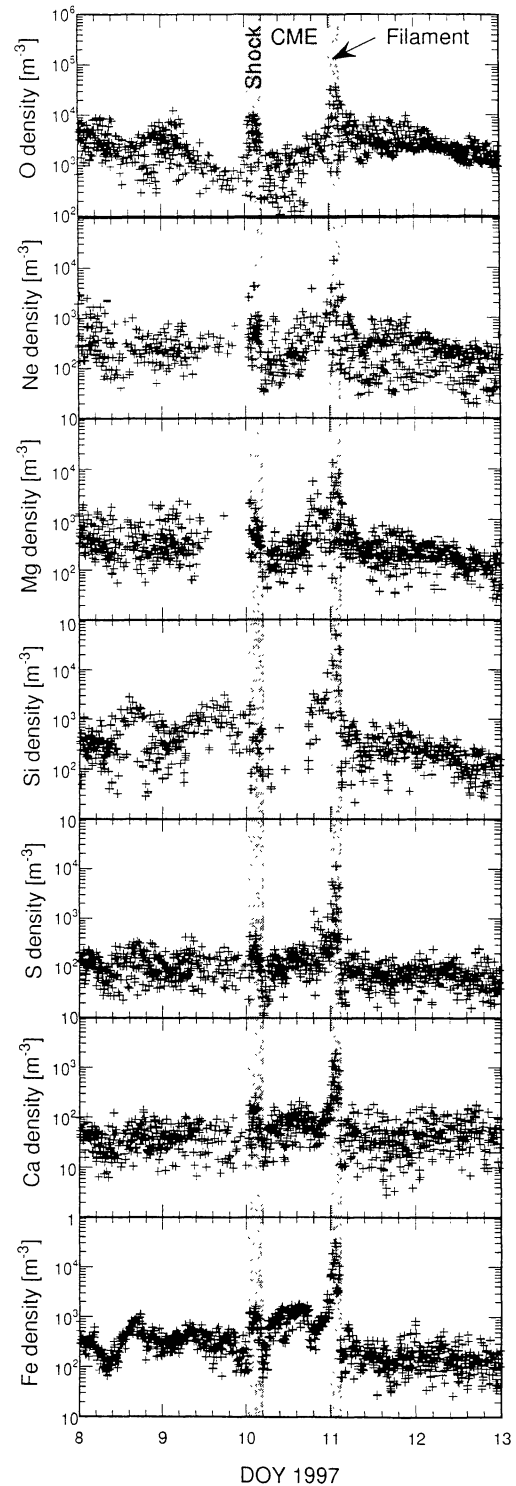


Figure 2: Densities for the different elements for the time period around the CME event. Each data point represents a measurement of 5 minutes. No smoothing of the data has been applied.

Table 1: Measured densities of some elements before, during, and after the CME event, with the exact time of the evaluated period given in days, starting January 1, 1997. Densities are given in m^{-3} , the quoted errors are statistical only.

Location	Time	n[O]	n[Ne]	n[Mg]	n[Si]	n[S]	n[Ca]	n[Fe]
Interstream	8.000–8.9934	2170±100	477±51	308±19	346±27	92.0±3.6	29.1±1.3	246±10
Compressed	10.022–10.183	3230±360	930±230	417±61	318±71	131±12	57.5±6.3	539±45
CME	10.253–10.896	874±73	384±71	274±49		105.8±7.2	54.1±2.4	631±24
filament	11.008–11.102	9760±2500	3100±1300	2220±680	13200±4800	1480±430	456±75	8460±1400
coronal hole	11.298–12.991	1896±56	274±11	149.4±4.6	162.9±6.5	54.4±1.5	35.4±1.6	117.6±3.8

Table 2: Abundance ratios of investigated elements with respect to oxygen. The error bars include statistical errors and instrumental errors. The photospheric abundance values were taken from [Anders and Grevesse, 1989, Grevesse and Anders, 1991].

Location	Time	n[Ne] / n[O]	n[Mg] / n[O]	n[Si] / n[O]	n[S] / n[O]	n[Ca] / n[O]	n[Fe] / n[O]
Photosphere		0.144±0.036	0.0447±0.0055	0.0417±0.0051	0.0191±0.0028	0.0027±0.0002	0.0355±0.0025
Interstream	8.000–8.9934	0.222±0.076	0.142±0.037	0.160±0.044	0.042±0.010	0.0134±0.0032	0.114±0.021
Compressed	10.022–10.183	0.29±0.16	0.129±0.052	0.099±0.048	0.041±0.014	0.0178±0.0066	0.167±0.049
CME	10.253–10.896	0.44±0.21	0.31±0.13		0.122±0.037	0.062±0.017	0.73±0.16
filament	11.008–11.102	0.32±0.28	0.23±0.16	1.4±1.0	0.15±0.11	0.047±0.027	0.87±0.45
coronal hole	11.298–12.991	0.146±0.039	0.079±0.017	0.086±0.019	0.029±0.006	0.0186±0.0042	0.062±0.010

(FIP), the FIP being less than about 10eV (e.g. the elements Mg, Si, Ca, and Fe in our study), was enhanced by a factor of about 4 in the interstream regime compared to the photospheric value. The enhancement amounted to only a factor of two in the coronal hole associated solar wind for low-FIP elements. For Ne, a high-FIP element, we found a small enrichment by a factor of 1.5 in the interstream regime and we found photospheric abundances in the coronal hole associated solar wind. This organization of the abundance of elements in the solar wind compared to their photospheric abundance by their FIP is the well-known FIP effect [Feldman, 1992, Marsch et al., 1995, Meyer, 1993]; however, the FIP effect is not yet fully understood [von Steiger, 1995]. Our data agree well with published data on elemental abundances in the solar wind. A plot of our data in the usual format is displayed in the upper panel of Figure 3. For Ca we found a larger enrichment in the interstream regime than for the other low-FIP elements. This agrees with the coronal abundance of Ca obtained from measurements of solar energetic particles (SEP) [Reames, 1992]. The enhancement of the Ca abundance in the coronal hole type solar wind is much larger than is expected for a low-FIP element. The Ca density practically remained the same in the interstream and in the coronal hole regime. Since Ca has such a low FIP it will be well ionized already in the chromosphere. Thus the requirement of an element being neutral in the chromosphere for the FIP fractionation effect to occur is not fulfilled. We are not aware of any published data on Ca abundances from other solar wind measurements. Due to the high efficiency and high mass resolution of MTOF, and the favorable observation conditions on

SOHO, we were able to measure the sulfur density with much improved time resolution compared to the only study reported until now for solar wind [Shafer et al., 1993]. In the framework of the FIP effect sulfur is an interesting element, because its ionization potential is approximately where one expects the transition between low-FIP and high-FIP elements to be. We found that sulfur is enriched in the slow solar wind by a factor of 2 compared to the photospheric abundance, and almost reached the photospheric value for coronal hole type solar wind. Thus sulfur is indeed in the transition between low and high FIP elements. For the $n[\text{S}]/n[\text{Si}]$ abundance ratio we found values of 0.27 ± 0.08 and 0.33 ± 0.09 for the interstream and the coronal hole associated solar wind, respectively. Considering the quoted errors, this is in reasonable agreement with the values 0.30 ± 0.12 and 0.40 ± 0.15 , respectively, from the earlier study [Shafer et al., 1993].

In the compressed region after the shock and before the CME, the densities of all elements increased somewhat (factors between 1.5 and 2.2) compared to their densities in the interstream region, the only exception being silicon, which remained at its value. There seemed to be a slight mass dependence, with the heavier elements showing more increase in density than the lighter ones. Notably, the iron density went up by a factor of more than two compared to its interstream value. Thus, the abundance ratios relative to oxygen showed this increase also, in particular for the heavier elements. However, the abundance ratio increase was still inside most of the error bars, since only a short time interval was available for integration in the compressed region. In principle, the compressed region

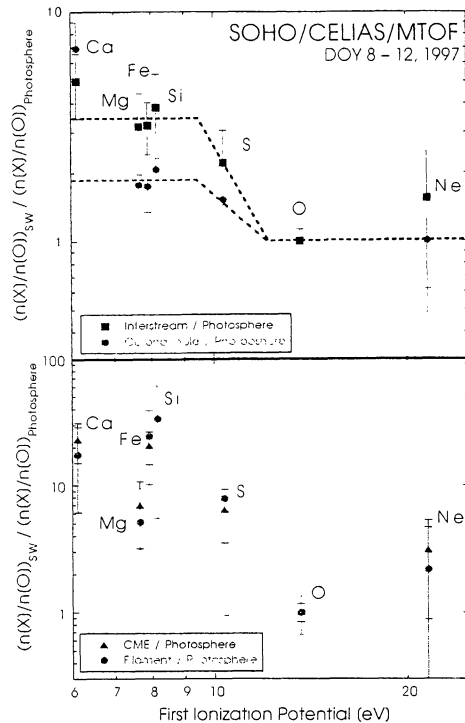


Figure 3: Solar wind abundance ratios for slow and fast solar wind (relative to oxygen) compared to photospheric ratios are plotted as a function of FIP. In the lower panel the same is done for the abundance ratios for the passage of the CME and the filament.

should be of the same elemental composition as the interstream solar wind.

For the CME we observed a markedly different composition compared to the interstream solar wind. Lower mass elements—and especially oxygen—appeared to be depleted, whereas heavier elements were enriched compared to their interstream densities (see Table 1 and upper panel in Figure 4). No such correlation was found between the abundance and the FIP (see lower panel in Figure 3). Unfortunately, no meaningful density value for silicon could be derived for the time period of the CME passage. In the MTOF sensor the incoming highly charged solar wind ions exchanged their charge to become single and doubly charged ions, which then were registered by the sensor. The $^{28}\text{Si}^+$ peak was contaminated with the $^{56}\text{Fe}^{++}$ mass peak in the recorded mass spectra, and the latter had to be subtracted from the former to derive the Si density. If the solar wind parameters are such that the instrument response is low for Si and high for Fe, which was the case for the CME period, such a correction is not possible and a meaningful Si density cannot be derived. Looking at the elemental abundances with respect to oxygen (see Table 2), a clear correlation between the mass and the abundance ratio with respect to oxygen was found. For the Ne/O abundance ratio an enrichment of a factor of 1.5 was found. The enrichment increased monotonically

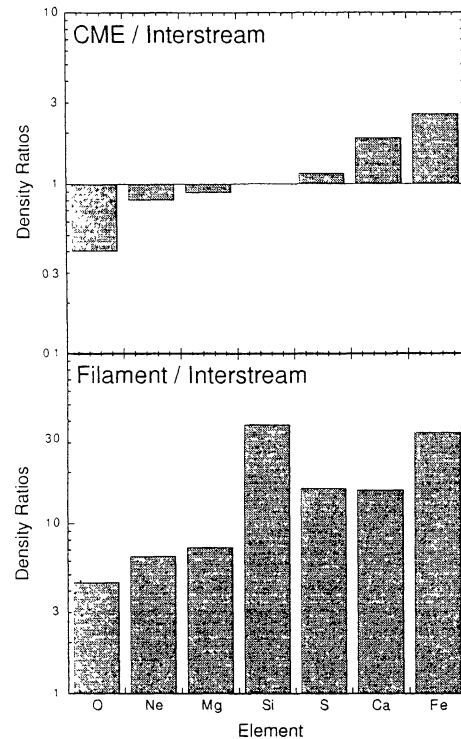


Figure 4: Ratio of densities during the CME and filament passage compared to the density in the interstream regime is given for the different elements. No value is given for Si in the upper panel.

with mass up to a factor of 7 for the Fe/O abundance ratio.

In the filament the densities of the heavier elements increased dramatically compared to their interstream values. A similar increase in density has also been observed for the protons [Burlaga, 1997]. Again we observed a clear mass dependence such as was found for the CME period (see Table 1 and lower panel of Figure 4). Only silicon deviated markedly from the otherwise monotonic increase of the abundance with mass. For the O density we observed an increase by a factor of 5. On the high mass side we observed an increase by a factor of 35 for the Si and Fe densities. Again, the increase in density cannot be correlated with the FIP.

In order to explain the unusual composition we found for the CME and filament material we could envisage a bubble of material, the precursor for the CME and the erupting filament, residing on the solar surface where matter boils off from the bubble. Given the gravitational field of the sun, lighter elements would boil off more easily than heavier ones and a mass-dependent change of composition would result if the bubble was reasonably isolated for a sufficiently long time on the solar surface. Once this bubble was released into space in the form of a CME or an erupting filament, it would carry with it the altered compositional information we observed in our data. Another explanation for these un-

usual compositions could be fractionation by shock acceleration. The mass-dependence we found for the elemental abundance during the CME and during the filament eruption could as well be interpreted as a mass-per-charge dependence. Inferring the charge from the type of solar wind (since MTOF determines only the mass of ions), we also obtained a monotonic function for the increase of the elemental abundance with mass per charge during these time periods. ^3He -rich flares, i.e. impulsive flares, usually also show enhancements of heavy elements, with Fe/O abundance ratios up to one [Meyer, 1985, Reames, 1992]. This enhancement is monotonic with mass, and is also called "mass bias", and results from the ion acceleration process that depends on the mass per charge of an ion as well as its velocity. However, whether the low energies (typically 1keV/nuc) of the particles we observed is enough that during the acceleration process to these energies the observed change in composition due to fractionation can be achieved is questionable.

ACKNOWLEDGMENTS

The authors are grateful to R. Neukomm and R. Wimmer-Schweingruber, both at University of Bern, for stimulating discussions on this topic. This work was supported by the Swiss National Science Foundation.

REFERENCES

- Anders, E. and Grevesse, N., "Abundances of elements: Meteoritic and solar," *Geochim. Cosmochim. Acta* **53**, 197-214 (1989).
- Burlaga, L.F., "Interplanetary stream interfaces," *J. Geophys. Res.* **86**, 3717-3725 (1974).
- Burlaga, L.F., ISTEP WWW page for the January 1997 CME event, 1997.
- Feldman, U., "Elemental abundances in the upper solar atmosphere," *Physica Scripta* **46**, 202-220 (1992).
- Grevesse, N. and Anders, E., "Solar Element Abundances," in *Solar Interior and Atmosphere*, Tucson, Univ. of Arizona Press, 1227-1234 (1991).
- Hamilton, D.C., Gloeckler, G., Ipavich, F.M., Lundgren, R.A., Sheldon, R.B., and Hovestadt, D., "New high resolution electrostatic ion mass analyzer using time of flight," *Rev. Sci. Instr.* **61**, 3104-3106 (1990).
- Hovestadt, D., Hilchenbach, M., Bürgi, A., Klecker, B., Laeverenz, P., Scholer, M., Grünwaldt, H., Axford, W.I., Livi, S., Marsch, E., Wilken, B., Winterhoff, P., Ipavich, F.M., Bedini, P., Coplan, M.A., Galvin, A.B., Gloeckler, G., Bochsler, P., Balsiger, H., Fischer, J., Geiss, J., Kallenbach, R., Wurz, P., Reiche, K.-U., Gliem, F., Judge, D.L., Hsieh, K.H., Möbius, E., Lee, M.A., Managadze, G.G., Verigin, M.I., and Neugebauer, M., "CELIAS: The Charge, Element, and Isotope Analysis System for SOHO," *Solar Physics* **162**, 441-481 (1995).
- Ipavich, F.M., Galvin, A.B., Lasley, S.E., Paquette, J.A., Hefti, S., Reiche, K.-U., Coplan, M.A., Gloeckler, G., Bochsler, P., Hovestadt, D., Grünwaldt, H., Hilchenbach, M., Gliem, F., Axford, W.I., Balsiger, H., Bürgi, A., Geiss, J., Hsieh, K.C., Kallenbach, R., Klecker, B., Lee, M.A., Managadze, G.G., Marsch, E., Möbius, E., Neugebauer, M., Scholer, M., Verigin, M.I., Wilken, B., and Wurz, P., "The Solar Wind Proton Monitor on the SoHO Spacecraft," *J. Geophys. Res.*, (1997) in press.
- Marsch, E., von Steiger, R., and Bochsler, P., "Element fractionation by diffusion in the solar chromosphere," *Astron. Astrophys.* **301**, 261-276 (1995).
- Meyer, J.P., "The baseline composition of solar energetic particles," *Astrophys. J. Suppl. Ser.* **57**, 151-171 (1985).
- Meyer, J.P., "Element fractionation at work in the solar atmosphere," in *Origin and Evolution of the Elements*, edited by N. Prantzos, E. Vangioni-Flam, and M. Cassè, Cambridge Univ. Press, Oxford, pp. 26-62, (1993).
- Reames, D.V., "Energetic particle observations and the abundance of elements in the solar corona," *ESA SP-348*, 315-323 (1992).
- Shafer, C.M., Gloeckler, G., Galvin, A.B., Ipavich, F.M., Geiss, J., von Steiger, R., and Ogilvie, K., "Sulfur abundances in the solar wind measured by SWICS on ULYSSES," *Adv. Space Res.* **13**, 79-82 (1993).
- von Steiger, R., "Solar wind composition and charge states," in *Solar Wind Eight*, Dana Point, Ca, USA, AIP Conference Proceedings, **382**, 193-198 (1995).